COMMUNICATION

Efficient, symmetric oligomer hole transporting materials with different cores for high performance perovskite solar cells†

Hyeju Choi,[a] Sojin Park,[a] Moon-Sung Kang[b] and Jaejung Ko*[a]

Novel symmetric oligomer hole transporting materials (HTMs) incorporating 3,4-ethylenedioxythiophene (EDOT) and 2,1,3-benzothiadiazole (BTD) cores have been synthesized and tested for high performance perovskite solar cells. A maximum energy conversion efficiency of 14.23% has been achieved by employing DPEDOT-B[BMPDP]₂ with the electron donating EDOT unit as the core, which is comparable to that of the traditional spiro-OMeTAD (14.55%).

Organometal halide perovskites ($CH_3NH_3PbX_3$, X = Cl, Br, I) possess special features, such as a direct band gap and intense light harvesting ability.[1] Thereby they can be utilized as both efficient light absorbers and electron–hole transporting materials for thin-film organic–inorganic hybrid solar cells.[2] Therefore, organometal halide perovskite solar cells have been recently receiving great attention owing to their outstanding features such as high efficiency and low cost.[3] In the perovskite solar cells, hole transporting materials (HTMs) play a key role in determining the photovoltaic performance. In this regard, the development of cost-effective and efficient HTMs is urgently needed. The most effective HTM for the hybrid solar cells is 2,2′,7,7′-tetrakis(*N,N*-di-*p*-methoxyphenyl-amine)-9,9′-spirobifluorene (**spiro-OMeTAD**) in terms of the efficiency and stability.[4] However, **spiro-OMeTAD** is quite expensive owing to the difficulty in its purification. For commercial purposes, the exploration of alternative HTMs with high performance and cheap synthetic price is strongly required. Recently, impressive photovoltaic performance has been achieved using small molecule HTMs, such as azomethine-,[5] 3,4-ethylenedioxythiophene-,[6] pyrene-,[7] linear π-conjugated-,[8] butadiene-,[9] **spiro-OMeTAD** derivative-,[10] carbazole derivative-,[11] tetrathiafulvalene-,[12] tetraphenyl-benzidine-,[13] oligothiophene

derivative-,[14] and spiro-thiophene derivative-[15] based HTMs showing efficiencies in the range of 10–15%. Recently, we[16] have reported quinolizino acridine-, star-shaped triphenylamino-, and triazine based HTMs, exhibiting high conversion efficiencies of ∼14%. Nevertheless, most of the small molecule HTMs are still expensive, with low conversion efficiency and low stability compared to **spiro-OMeTAD**. Therefore, the development of cheap HTMs with operation stability is still very important.

Herein, we report three types of hole transporting materials by incorporating an electron donating unit or an electron-withdrawing unit into tetraphenyl benzidine or substituting four triphenylamines into the phenyl unit. The molecular structures of the three HTMs are shown in Fig. 1.

The synthetic scheme for the preparation of **B[BMPDP]₂**, **DPEDOT-B[BMPDP]₂** and **DPBTD-B[BMPDP]₂** is shown in Scheme 1. The primary step for their syntheses is the Suzuki coupling reaction[17] of bis(4-bromophenyl)amine and *N*-bis-(methoxyphenyl)-*N*-(4-(4,4,5,5,-tetramethyl-1,3,2-dioxaborolan-2-yl)phenyl)amine. The final two HTMs were synthesized by the Buchwald–Hartwig amination[18] of **1** and dihalo derivatives.

The UV-vis absorption spectra of the three HTMs recorded in chlorobenzene are displayed in Fig. 2a. As summarized in Table S1 (ESI†), the UV-vis light absorption peaks of **B[BMPDP]₂**, **DPEDOT-B[BMPDP]₂** and **DPBTD-B[BMPDP]₂** were observed at 376, 377, and 473 nm, respectively. The λ_{abs} of **DPBTD-B[BMPDP]₂** is more red shifted than that of **DPEDOT-B[BMPDP]₂**. This bathochromic shift seems to be attributed to an intramolecular charge transfer in

Fig. 1 Chemical structures of **B[BMPDP]₂**, **DPEDOT-B[BMPDP]₂** and **DPBTD-B[BMPDP]₂** moieties studied in the present work.

[a] *Department of Advanced Material Chemistry, Korea University Sejong Campus, Sejong-ro 2511, Sejong City 339-700, Republic of Korea. E-mail: jko@korea.ac.kr; Fax: +82-41-867-1331; Tel: +82-41-860-1337*

[b] *Department of Environmental Engineering, Sangmyung University, 300 Anseo-dong, Dongnam-gu, Cheonan-si, Chungnam 330-720, Republic of Korea*
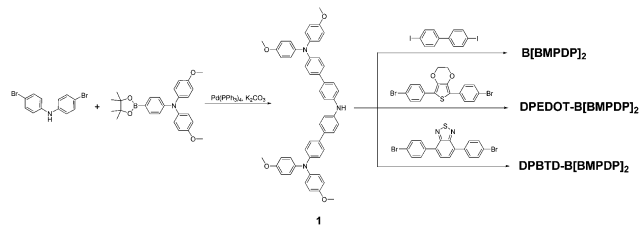
Scheme 1 Schematic diagram for the synthesis of **B[BMPDP]₂**, **DPEDOT-B[BMPDP]₂** and **DPBTD-B[BMPDP]₂**.

Fig. 2 (a) Absorption and emission spectra of the HTMs in chlorobenzene. Inset: UV-vis absorption spectra of the HTMs coated on mp-TiO₂/MAPbI₃ films. (b) Cross-sectional field-emission scanning electron microscopy (FE-SEM) image of mp-TiO₂/MAPbI₃/HTM/Au. (c) Energy level diagram of each component.

Fig. 3 (a) Photocurrent–voltage (J–V) curves of the solar cells with **B[BMPDP]₂** (■), **DPEDOT-B[BMPDP]₂** (●), **DPBTD-B[BMPDP]₂** (▲) and **spiro-OMeTAD** (◆) as the HTMs, respectively. (b) Corresponding IPCE spectra.

DPBTD-B[BMPDP]₂. The fluorescence spectra of **B[BMPDP]₂** and **DPEDOT-B[BMPDP]₂** exhibit an emission at 429 and 472 nm with a small Stokes shift of 53–95 nm compared with a large Stokes shift of 175 nm in **DPBTD-B[BMPDP]₂**, demonstrating that a small structural change in the excited state occurs in the two former compounds. The inset of Fig. 2a shows the absorption spectra of the perovskite-coated mesoporous TiO₂ films with the three HTMs. Three HTM-coated films exhibit an enhanced absorption band from 350 to 580 nm.
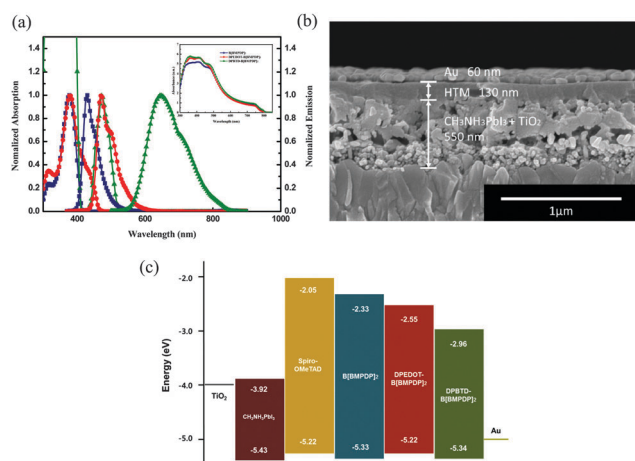
The cross-sectional field-emission scanning electron microscopy (FE-SEM) image of the prepared perovskite solar cell is displayed in Fig. 2b, showing a well-defined multi-layer structure with clear interfaces. The thickness of the TiO₂ scaffold film incorporated with perovskite, HTM layer and Au is 550 nm and 130 nm and 60 nm, respectively. Fig. 2c shows a comparative diagram of the energy levels of the corresponding components in the device. The HOMO levels of **B[BMPDP]₂**, **DPEDOT-B[BMPDP]₂** and **DPBTD-B[BMPDP]₂** are measured to be −5.33, −5.22 and −5.34 eV, respectively, which are well matched with CH₃NH₃PbI₃ (−5.43 eV).

Fig. 3a shows the photocurrent–voltage (J–V) curves of the perovskite solar cells employing the HTMs. For reference, the device with **spiro-OMeTAD** as the HTM is fabricated. The detailed photovoltaic parameters of the devices are also summarized

in Table 1. We have fabricated 30 solar cells for each HTM and the histogram of energy conversion efficiencies for the cells is shown in Fig. S3 (ESI†). The energy conversion efficiencies of the cells employing three HTMs were shown to be almost comparable with that of the **spiro-OMeTAD** based reference cell. The average efficiencies for **B[BMPDP]₂**, **DPEDOT-B[BMPDP]₂**, and **DPBTD-B[BMPDP]₂** and **spiro-OMeTAD** were observed to be 12.37, 13.12, 13.09, and 13.43%, respectively.

The highest energy conversion efficiency (14.23%) was achieved by employing the **DPEDOT-B[BMPDP]₂** under one sun illumination. The incident photon-to-current efficiency (IPCE) spectra of

Table 1 Summary of photovoltaic parameters of the solar cells employing different HTMs

HTM		J_{sc} (mA cm⁻²)	V_{oc} (V)	FF	η (%)
B[BMPDP]₂	Average	20.69	0.938	0.637	12.37
	Best	21.29	0.972	0.667	13.81
DPEDOT-B[BMPDP]₂	Average	20.87	0.955	0.660	13.12
	Best	21.07	0.947	0.713	14.23
DPBTD-B[BMPDP]₂	Average	20.69	0.965	0.657	13.09
	Best	20.96	0.951	0.702	13.99
spiro-OMeTAD	Average	20.82	0.939	0.688	13.43
	Best	21.17	1.003	0.685	14.55

Performances of devices were measured with 0.16 cm² working area.

the solar cells fabricated with three HTMs are shown in Fig. 3b. The integrated photocurrent densities of the cells employing **B[BMPDP]₂**, **DPEDOT-B[BMPDP]₂**, and **DPBTD-B[BMPDP]₂** were calculated to be 19.54, 19.92 and 19.76 mA cm^{-2}, respectively, which are well consistent with the measured photocurrent densities as summarized in Table 1. The **DPBTD-B[BMPDP]₂** based cell shows a slightly high open circuit voltage (V_{oc}) compared with those of other two cells, which can be rationalized by considering that the E_{HOMO} for **DPBTD-B[BMPDP]₂** was about 10–120 mV lower than the value for the other two cells. The similar and slight differences of J_{sc} value of three cells in different wave-length ranges may be related to their low series resistance (R_s) due to their packing patterns. From the slope of the J–V curve around V_{oc}, the R_s values of **B[BMPDP]₂**, **DPEDOT-B[BMPDP]₂**, and **DPBTD-B[BMPDP]₂** based cells are calculated to be 26.4, 22.6 and 23.8 Ω cm^{-2}, respectively, in which the low value of R_s in **DPEDOT-B[BMPDP]₂** leads to slightly improved photocurrent density. The high fill factors in the **DPEDOT-B[BMPDP]₂** based cell followed a trend identical to the measured value in mobility. The hole mobilities of the HTMs were measured from the space charge limitation of current (SCLC) in the J–V characteristics. The hole mobilities evaluated by the Mott–Gurney law[19] in **B[BMPDP]₂**, **DPEDOT-B[BMPDP]₂**, **DPBTD-B[BMPDP]₂** and **spiro-OMeTAD** are 7.04×10^{-5}, 8.48×10^{-5}, 8.05×10^{-5}, 1.01×10^{-4} cm^2 V^{-1} s^{-1}, respectively. The high hole mobilities of **DPEDOT-B[BMPDP]₂** and **DPBTD-B[BMPDP]₂** based cells relative to that of the **B[BMPDP]₂** based one led to an improved fill factor.

Electrochemical impedance spectroscopy measurements have also been carried out to analyse the recombination properties of the HTMs. The Nyquist plots of the devices with **B[BMPDP]₂**, **DPEDOT-B[BMPDP]₂**, and **DPBTD-B[BMPDP]₂** in the dark over different forward biases (600–1000 mV) are shown in Fig. S5 (ESI†). The magnitude of the main arc is dominated by the recombination resistance (R_{rec}), which drops with the increasing forward bias voltage. The R_{rec} values were shown to be significantly increased under identical bias conditions upon introducing the EDOT and BTD core units into HTMs, demonstrating the decrease in the charge recombination. These results are also well consistent with the V_{oc} values evaluated from the J–V curves.

Fig. 4 shows the photovoltaic performance during the long-term aging test of the two devices. After 200 h of aging, the initial efficiency of 12.55% of the **DPEDOT-B[BMPDP]₂** based cell decreased to 11.01%, giving a 12.55% reduction. On the other hand, the initial efficiency of 13.55% of the **spiro-OMeTAD** based cell also decreased to 12.57%, giving a 7.23% reduction. The relative stability of the **DPEDOT-B[BMPDP]₂** based cell may be attributable to an interfacial tight packing due to a planar and sterically bulky configuration.

In summary, we have designed and synthesized three novel HTMs with 3,4-ethylenedioxythiophene (EDOT) and 2,1,3-benzo-thiadiazole (BTD) as the core units. The photo-physical properties and photovoltaic performance are quite sensitive to the structural configuration. The **DPEDOT-B[BMPDP]₂** based cell affords an overall conversion efficiency of 13.12%, showing a

Fig. 4 Time-course changes in the performance parameters of the solar cells with **DPEDOT-B[BMPDP]₂** (●) and **spiro-OMeTAD** (♦) as the HTMs under inert conditions at room temperature.

comparable photovoltaic performance to the **spiro-OMeTAD** based cell (13.43%). We believe that the development of efficient and stable hole transporting materials comparable to the **spiro-OMeTAD** is possible through meticulous molecular design, and studies directed towards this goal are now in progress.

Notes and references

1 M. Liu, M. B. Johnston and H. J. Snaith, *Nature*, 2013, **501**, 395; L. Etgar, P. Gao, Z. Xue, Q. Peng, A. K. Chandiran, B. Liu, M. d. K. Nazeeruddin and M. Grätzel, *J. Am. Chem. Soc.*, 2012, **134**, 17396.
2 L. Etgar, P. Gao, Z. Xue, Q. Peng, A. K. Chandiran, B. Liu, M. K. Nazeeruddin and M. Grätzel, *J. Am. Chem. Soc.*, 2012, **134**, 17396.
3 H.-S. Kim, C.-R. Lee, J.-H. Im, K.-B. Lee, T. Moehl, A. Marchioro, S.-J. Moon, R. Humphry-Baker, J.-H. Yum, J. E. Moser, M. Grätzel and N.-G. Park, *Sci. Rep.*, 2012, **2**, 591; J.-H. Yum, C.-R. Lee, J.-W. Lee, S.-W. Park and N.-G. Park, *Nanoscale*, 2011, **3**, 4088.
4 J. Burschka, N. Pellet, S.-J. Moon, R. Humphry-Baker, P. Gao, M. K. Nazeeruddin and M. Grätzel, *Nature*, 2013, **499**, 316; D. Liu and T. L. Kelly, *Nat. Photonics*, 2014, **8**, 133.
5 M. L. Petrus, T. Bein, T. J. Dingemans and P. Docampo, *J. Mater. Chem. A*, 2015, **3**, 12159.
6 H. Li, K. Fu, A. Hagfeldt, M. Grätzel, S. G. Mhaisalkar and A. C. Grimsdale, *Angew. Chem., Int. Ed.*, 2014, **53**, 4085.
7 N. J. Jeon, J. Lee, J. H. Noh, M. K. Nazeeruddin, M. Grätzel and S. I. Seok, *J. Am. Chem. Soc.*, 2013, **135**, 19087.
8 J. Wang, S. Wang, X. Li, L. Zhu, Q. Meng, Y. Xiao and D. Li, *Chem. Commun.*, 2014, **50**, 5829.
9 S. Lv, L. Han, J. Xiao, L. Zhu, J. Shi, H. Wei, Y. Xu, J. Dong, X. Xu, D. Li, S. Wang, Y. Luo, Q. Meng and X. Li, *Chem. Commun.*, 2014, **50**, 6931.
10 N. J. Jeon, H. G. Lee, Y. C. Kim, J. Seo, J. H. Noh, J. Lee and S. I. Seok, *J. Am. Chem. Soc.*, 2014, **136**, 7837.
11 B. Xu, E. Sheibani, P. Liu, J. Zhang, H. Tian, N. Vlachopoulos, G. Boschloo, L. Kloo, A. Hagfeldt and L. Sun, *Adv. Mater.*, 2014, **26**, 6629; S. D. Sung, M. S. Kang, I. T. Choi, H. M. Kim, H. Kim, M. P. Hong, H. K. Kim and W. I. Lee, *Chem. Commun.*, 2014, **50**, 14161.
12 J. Liu, Y. Wu, C. Qin, X. Yang, T. Yasuda, A. Islam, K. Zhang, W. Peng, W. Chen and L. Han, *Energy Environ. Sci.*, 2014, **7**, 2963.

13 Y. Song, S. Lv, X. Liu, X. Li, S. Wang, H. Wei, D. Li, Y. Xiao and Q. Meng, *Chem. Commun.*, 2014, **50**, 15239.

14 L. Zheng, Y.-H. Chung, Y. Ma, L. Zhang, L. Xiao, Z. Chen, S. Wang, B. Qu and Q. Gong, *Chem. Commun.*, 2014, **50**, 11196.

15 S. Ma, H. Zhang, N. Zhao, Y. Cheng, M. Wang, Y. Shen and G. Tu, *J. Mater. Chem. A*, 2015, **3**, 12139.

16 P. Qin, S. Peak, M. I. Dar, N. Pellet, J. Ko, M. Grätzel and M. K. Nazeeruddin, *J. Am. Chem. Soc.*, 2014, **136**, 8516; K. Do, H. Choi, K. Lim, H. Jo, J. W. Cho, M. K. Nazeeruddin and J. Ko, *Chem. Commun.*, 2014, **50**, 10971; H. Choi, S. Park, S. Paek, P. Ekanayake, M. K. Nazeeruddin and J. Ko, *J. Mater. Chem. A*, 2014, **2**, 19136; H. Choi, S. Paek, N. Lim, Y. H. Lee, M. K. Nazeeruddin and J. Ko, *Chem. – Eur. J.*, 2014, **20**, 10894.

17 C.-H. Huang, N. D. McClenaghan, A. Kuhn, J. W. Hofstraat and D. M. Bassani, *Org. Lett.*, 2005, **7**, 3409; K. J. Hoffmann, E. Bakken, E. J. Samuelsen and P. H. J. Carlsen, *Synth. Met.*, 2000, **113**, 39.

18 N. Cho, H. Choi, D. Kim, K. Song, M.-S. Kang, S. O. Kang and J. Ko, *Tetrahedron*, 2009, **65**, 6236.

19 V. D. Mihailetchi, H. Xie, B. de Boer, L. J. A. Koster and P. W. M. Blom, *Adv. Funct. Mater.*, 2006, **16**, 699.